Available online at www.sciencedirect.com
ScienceDirect
Journal of Sound and Vibration 306 (2007) 928–939
JOURNAL OF SOUND AND VIBRATION
www.elsevier.com/locate/jsvi

A natural way for improving the accuracy of the continuous wavelet transforms

Wen-xian Yang*

Institute of Vibration Engineering, Northwestern Polytechnical University, Xi'an, 710049, China

Received 24 August 2006; received in revised form 25 June 2007; accepted 2 July 2007

Abstract

Aiming at further increasing the accuracy of the continuous wavelet transforms (CWTs) of transient vibration signals, a new coefficient trimming technique is proposed in this paper. Different from the conventional CWT analysis, which treats different scales of daughter wavelets equally and without using any discrimination, the proposed technique takes the role of the daughter wavelet into account in the CWT calculations. In the concept of this new technique, not only different scales of daughter wavelets play different roles in the calculations, but also the daughter wavelet at the same scale also plays a different role at different time instants. The role of the daughter wavelet is numerically evaluated through the approach of the correlation between the daughter wavelet and the instant signal within the time-sliding window, which window length is predefined by using a compromise strategy. Once the correlation coefficient indicating the role of a daughter wavelet at certain time instant is obtained, it will be applied to trim the corresponding CWT coefficient that is derived at the corresponding wavelet scale and the current time instant. The details of this operation are given in the following context of the paper. Extensive experiments show that with the aid of this proposed technique, the false information in the CWT map is successfully removed, while the true information of the vibration signal is retained sufficiently. Moreover, different from the threshold-based purification methods, the continuity and the smoothness of the wavelet coefficients are maintained perfectly in the whole process. So the results obtained by using the proposed technique are more explicit and reliable, from which the signal features may be identified more easily and correctly. This is very helpful for promoting understanding of the dynamic behaviour of the machines and furthermore giving a more reliable assessment of their running condition.

1. Introduction

Since 1980s [1] and especially since Daubechies laid down the mathematical basis of wavelet analysis in her 'Ten Lectures on Wavelets' [2], the research on wavelets has grown exponentially. Various kinds of wavelet functions were specifically designed, such as Morlet, Daubechies, Haar, Gaussian, Mexican Hat, Coiflet, Symlet, Biorthogonal and so on. The details may be found from some overview literature [3–6]. In the meantime, the wavelet transform has been regarded as the most promising technique and extensively applied

*Corresponding author. Present address: Applied Mathematics & Computing Group, Department of Process and Systems Engineering, Cranfield University, Cranfield, MK43 0AL, UK.
E-mail address: w.yang@cranfield.ac.uk

0022-460X/$ - see front matter © 2007 Elsevier Ltd. All rights reserved.
doi:10.1016/j.jsv.2007.07.001

to a wide variety of fields such as signal processing, image processing, pattern recognition, seismology, machine visualisation, medical industry and atmospheric sciences. In the field of mechanical engineering, the continuous wavelet transform (CWT) is particularly interesting due to its multiple-resolution property and visual advantage in analysing vibration signals. Nowadays, the CWT has been successfully applied to crack detection [7], rolling bearing diagnosis [8], gear diagnosis [9], ultrasonic detection [10], identification of weak nonlinearities in structural damping and stiffness [11], etc. However, as the CWT adopts the matching mechanism between the wavelet function and the inspected signal to identify the signal features, the overlapping in frequency vicinities is inevitable in the results derived by using the CWT. This phenomenon has been explained in detail in Refs. [8,12,13]. In addition, the noise-induced structures, such as 'ripples', 'blips' and unidentified oscillations, are usually present in the CWT results. They smear the spectral features in the CWT map and give rise to interpretational difficulties. In consequence, they significantly limit the wider application of the CWT. In order to eliminate them, many efforts have been devoted. For example, Newland [14] proposed a method namely wavelet ridge extraction. Donoho [15] designed a soft-thresholding method for removing the redundant noise-induced structures from the CWT results. Tse and Yang [13] proposed an overlapping reduction method based on statistics and the maximum matching mechanism of wavelet transform. Unfortunately, all these methods disrupt the smoothness and the continuity of wavelet coefficients. Moreover, a reliable result can hardly be achieved by using these approaches, i.e. either false information caused by overlapping and noise may not be removed or true information is eliminated by mistake. In order to make up for the deficiency of these methods, Yang and Tse [16] developed a more flexible soft-thresholding method in terms of exponential functions. However, the operation of this method is complicated and moreover, the practice shows that it does not work very well when dealing with signals with multiple frequency components at the same time instant. In view of this situation further research is performed in this paper and a new technique based on the idea of correlation is proposed. In the implementation of this new technique, the role of the daughter wavelet at different wavelet scale is clearly discriminated from other possibilities, and the CWT results are purified based on this discrimination. By the means of this method, the undesired phenomena are removed successfully, while the true information in the signal is retained sufficiently in the meantime.

The structure of the paper is organised as follows. In Section 2, the theoretical background of the CWT and its correlation-based purification scheme are depicted. In Section 3, the determination of the length of the time window for correlation calculation is clearly explained. In Section 4, the proposed technique and its robust noise performance are examined by simulated experiments and through the comparison with other CWT trimming methods available today. In Section 5, the vibration signals collected from an engine valve gear system are analysed for demonstrating the successful application of the proposed technique in industry. The conclusions of the paper are given in Section 6.

2. Fundamental theory

For a given square-integrable signal $f(t) \in L^2(\Re)$ in the time domain $(-\infty, \infty)$, the continuous wavelet transform is the inner product of the signal with a series of daughter wavelet functions geometrically controlled by a dilatation (or scale) parameter a and a time translation (or shift) parameter b, i.e.

$$W_f(a,b) = \left\langle f, \psi^*_{a,b} \right\rangle = \frac{1}{\sqrt{a}} \int_{-\infty}^{\infty} f(t) \psi^* \left(\frac{t-b}{a} \right) \mathrm{d}t, \tag{1}$$

where $L^2(\Re)$ denotes the Hilbert space of measurable, square-integrable one-dimensional signals. $W_f(a,b)$ is a wavelet coefficient for the wavelet $\psi_{a,b}(t)$ and it measures the variation of the signal in the vicinity of the time $t = b$. The size of the vicinity is proportional to the scale parameter a, which defines the analysing window stretching. $\psi(t)$ represents a mother wavelet and the super star '*' indicates its complex conjugation. Its Fourier transform needs to satisfy the following admissibility condition:

$$c_\psi = \int_{-\infty}^{\infty} \frac{|\hat{\psi}(\omega)|^2}{|\omega|} \mathrm{d}\omega < +\infty, \tag{2}$$

where $\hat{\psi}(\omega)$ is the Fourier transform of $\psi(t)$. It follows that $\hat{\psi}(\omega)$ is a continuous function, so that the finiteness of c_ψ implies that $\hat{\psi}(0) = 0$ or the mean value of $\psi(t)$ in the time domain is zero, i.e. $\int_{-\infty}^{\infty} \psi(t)\,\mathrm{d}t = 0$.

This admissibility condition is necessary to obtain the inverse of the wavelet transform. Different from the Fourier transform whose decomposition does not give any local time information of the inspected signal, the wavelet $\psi(t)$ must also be a window function that simultaneously enables the possibility of time–frequency localisation. In other words, $\psi(t)$ must decay at infinity, i.e.

$$\int_{-\infty}^{\infty} |\psi(t)|\,\mathrm{d}t < +\infty. \tag{3}$$

Attributed to these properties of the defined wavelet, the CWT obtains the property of frequency localisation, which can be observed from the expression of the CWT in terms of the Fourier transform:

$$W_f(a,b) = \frac{\sqrt{a}}{2\pi}\int_{-\infty}^{\infty} \hat{f}(\omega)\hat{\psi}^*(a\omega)\mathrm{e}^{\mathrm{j}\omega b}\,\mathrm{d}\omega, \tag{4}$$

where $\hat{f}(\omega)$ is the Fourier transform of $f(t)$. Obviously, the frequency localisation of the CWT depends on the scale parameter a.

From Eq. (4), it is inferred that when the frequency of the daughter wavelet is close to the frequency of the signal, a big wavelet coefficient will be obtained. Moreover, the closer the two frequencies, the bigger is the coefficient. Conversely, the further apart the two frequencies, the smaller is the value of the coefficient. This is why we say that the CWT adopts a 'matching mechanism' between the wavelet function and the inspected signal to identify the time–frequency features of the signal. The disadvantage of adopting 'matching mechanism' is the appearance of overlapping at adjacent frequencies. Inspired by the knowledge that the better the daughter wavelet function matches the signal, the bigger the wavelet coefficient, one usually minimises the overlapping through threshold-based approaches. But these approaches often result in the disruption of the continuity and the smoothness of the wavelet coefficients. Moreover, as these methods cannot identify whether the information is true or false, the true information of the signal is often removed by mistake while the false information is incorrectly retained. In order to overcome this shortcoming, a new technique based on the idea of correlation is proposed in the paper. In the author's previous research, the role of the daughter wavelet at different scale is never taken into account in the CWT process. This is why one cannot always purify the CWT results correctly. In fact the different scale of the daughter wavelet plays a different role in the CWT process, i.e. in the sense of theory, only those daughter wavelets highly related to the inspected signal play vital roles, while those unrelated to the signal should not play important role because they create nothing but interference structures leading to misinterpretation of the signal. Therefore, how to discriminate the roles of daughter wavelets at different scales is critical for this technique.

'Correlation' is one of the most common and most useful statistical measures, which describes the degree of linear dependence between the two variables in terms of a coefficient between -1.0 and $+1.0$. The closer the coefficient is to either -1.0 or $+1.0$, the stronger the correlation between the two variables is. The negative and positive signs of the coefficient indicate the direction of the linear dependence. The coefficient 0 implies that the two variables are completely independent of each other. The correlation $\rho_{X,Y}$ between two random variables X and Y with expected values μ_X and μ_Y and standard deviations σ_X and σ_Y is defined as

$$\rho_{X,Y} = \frac{\mathrm{cov}(X,Y)}{\sigma_X\sigma_Y} = \frac{E((X-\mu_X)(Y-\mu_Y))}{\sigma_X\sigma_Y}, \tag{5}$$

where E is the expected value of the variable and 'cov' means covariance. Since $\mu_X = E(X)$, $\sigma_X^2 = E(X^2) - E^2(X)$ and likewise for Y, Eq. (5) can be also written as

$$\rho_{X,Y} = \frac{E(XY) - E(X)E(Y)}{\sqrt{E(X^2) - E^2(X)}\sqrt{E(Y^2) - E^2(Y)}}. \tag{6}$$

It is well known that when two signals have same or similar frequencies, a big value of correlation coefficient can always be obtained regardless of their amplitudes and phases. Inspired by this knowledge, the role of a daughter wavelet may be defined by the absolute value of the correlation coefficient between the inspected

signal f and a sinusoidal function H with the frequency corresponding to the present wavelet scale, i.e.

$$\gamma(a,t) = |\rho_{f(T),H(a,T)}(t)| = \left|\frac{\mathrm{cov}(f(T),H(a,T))}{\sigma_{f(T)}\sigma_{H(a,T)}}\right|, \tag{7}$$

where $T \in [t-\tau/2 \quad t+\tau/2]$, τ defines the time duration of the signal f and the function H used for calculation, a indicates the present wavelet scale. For those wavelets with a kernel function, e.g. the Morlet wavelet, the Gabor wavelet, and the Laplace wavelet, the function H is, in essence, the real part of the kernel function at the corresponding scale. For facilitating understanding, the functions H for the Morlet wavelet and the Gabor wavelet are derived in the following. The Morlet wavelet is formulated as

$$\psi(t) = \mathrm{e}^{-(t^2/2)\beta}\mathrm{e}^{(\mathrm{j}\omega_0 t)} \quad (\mathrm{j} = \sqrt{-1}, \quad \omega_0 \geqslant 5), \tag{8}$$

where β is a shape control parameter for the Gaussian window. The daughter Morlet wavelet at scale a can be written as

$$\psi(a,t) = \mathrm{e}^{-((t/a)^2/2)\beta}\mathrm{e}^{(\mathrm{j}\omega_0 t/a)}. \tag{9}$$

The corresponding function H is derived as follows:

$$H(a,T) = \mathrm{Re}(\psi(a,T)\,\mathrm{e}^{((T/a)^2/2)\beta}) = \sin\left(\frac{\omega_0}{a}T\right). \tag{10}$$

From Eq. (10), it is obviously seen that the function H for the Morlet wavelet is a sinusoidal function. This is in accordance with the statement given above. The equation of the Gabor wavelet is expressed as

$$\psi_{\mathrm{G}}(t) = G(\omega_0,t)\mathrm{e}^{\mathrm{j}\omega_0 t} \quad (\mathrm{j} = \sqrt{-1}), \tag{11}$$

where

$$G(\omega_0,t) = \frac{1}{\sqrt[4]{\pi}}\sqrt{\frac{\omega_0}{r}}\mathrm{e}^{-((\omega_0/r)^2/2)t^2}. \tag{12}$$

When $r = \pi\sqrt{2/\ln 2}$, $G(\omega_0,t)$ can be considered as a Gaussian window centred at $t = 0$. The function H for the daughter Gabor wavelet at scale a is derived as

$$H(a,T) = \mathrm{Re}\left(\frac{\psi_{\mathrm{G}}(T/a)}{G(\omega_0,T/a)}\right) = \sin\left(\frac{\omega_0}{a}T\right). \tag{13}$$

It is a sinusoidal function as well. The same result may also be derived from the Laplace wavelet.

The role of a daughter wavelet determines the reliability of the wavelet coefficients derived by using it. Hence, the CWT coefficients at scale a and time t may be trimmed through the equation

$$\hat{W}_f(a,b,t) = \gamma(a,t)\,W_f(a,b,t). \tag{14}$$

When dealing with a practical non-stationary vibration signal, the same scale of the daughter wavelet may play a different role at different times. Unfortunately, the correlation is a statistical measure. It is unable to describe instantaneous information. What we can do is only to evaluate the role of a daughter wavelet in a short time duration defined by a time window. Then, move the time window along the time axis to obtain the 'instantaneous' role of the daughter wavelet for the whole time duration of the signal.

3. Determination of the length of time window

As the correlation coefficient is a statistical measure, the statistical integrity should be considered in the determination of the length of time window. In other words, the window length should not be too short, otherwise the reliability of the derived correlation coefficient cannot be guaranteed. However, for the present application, using a big length of time window for correlation calculation is not in accordance with the concept of the wavelet transform, i.e. the derived results cannot describe the role of the daughter wavelet instantaneously. Therefore, it is necessary to design a compromise strategy to determine

the length of time window (i.e. τ in Eq. (7)). In order to meet this requirement, a method is proposed in this paper. For facilitating understanding of the proposed method, a simulated signal is employed. It is

$$X(t) = \sum_{i=1}^{5} \sin(\omega_i t) + n(t), \tag{15}$$

where $\omega_i = 2\pi f_i$, $f = [30 \quad 40 \quad 50 \quad 70 \quad 90]$ Hz, $t = 0$–1 s, and $n(t)$ represents white noise.

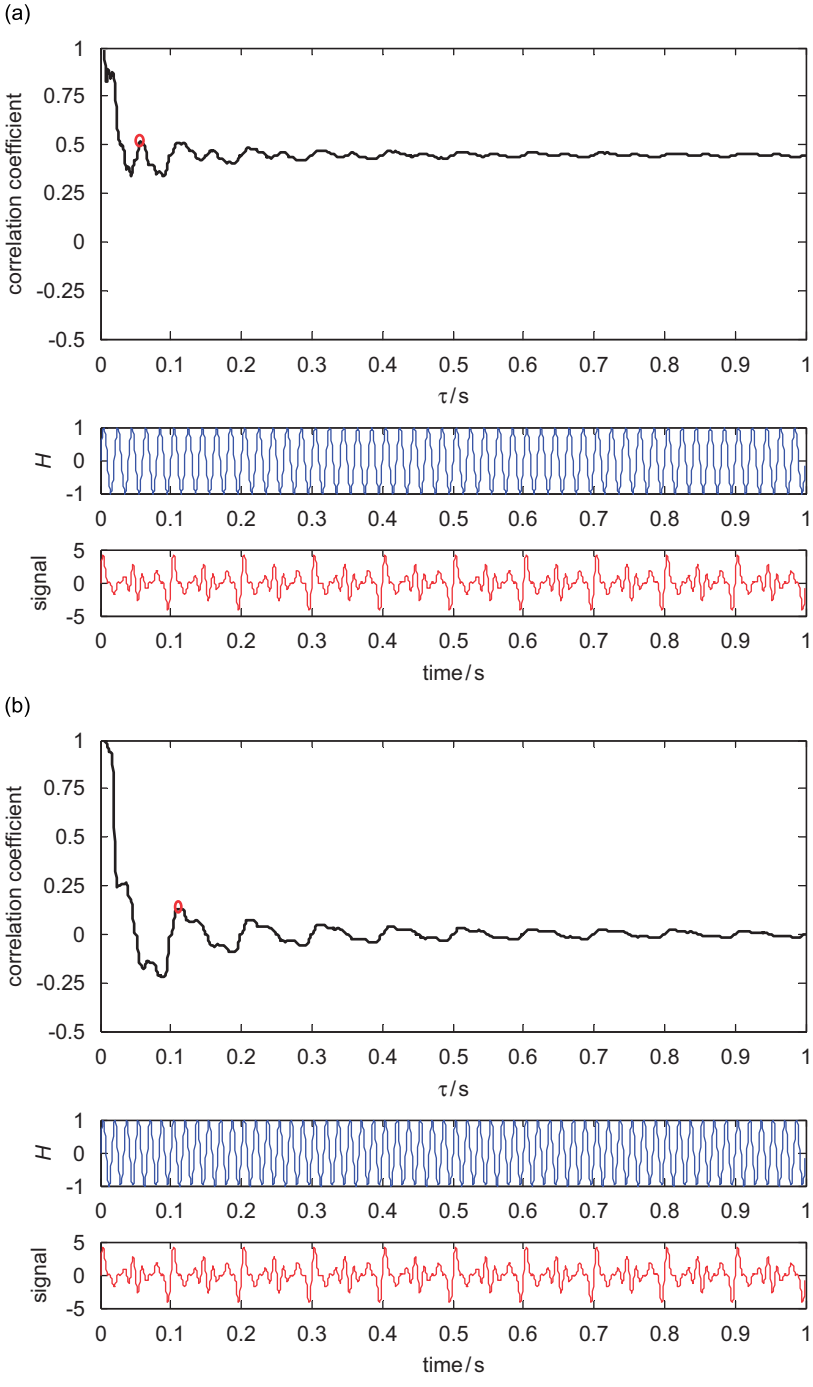

Fig. 1. Variation tendency of the correlation coefficient against τ: (a) when $\check{f}_a = 50$ Hz, (b) when $\check{f}_a = 60$ Hz.

Assume the function H corresponding to wavelet scale a is

$$H(a,T)=\sin(\breve{\omega}_a T), \tag{16}$$

where $T\in[t-\tau/2 \quad t+\tau/2]$ and $\breve{\omega}_{\mathrm{a}}=2\pi\breve{f}_a=\omega_0/a$.

Then the variation tendency of the correlation coefficient between the signal $X(t)$ and the function $H(t)$ is calculated against the increasing τ. The calculation results obtained when $\breve{f}_{\mathrm{a}}=50$ and 60 Hz are shown in Fig. 1.

From Fig. 1, it is seen that with the increasing τ, the correlation coefficient between $X(t)$ and $H(t)$ decays in an oscillatory way and finally converges toward an asymptotic value that indicates the true linear dependency between $X(t)$ and $H(t)$. When $\breve{f}_a$ matches one of the frequency components contained in the signal (e.g. when $\breve{f}_a=50$ Hz), the correlation coefficient shows a big asymptotic value, while it shows a very small asymptotic value if $\breve{f}_a$ does not match any frequency components in the signal (e.g. when $\breve{f}_a=60$ Hz). However, as stated above, we cannot use a big number of data in practical calculations, so the value of τ when the first peak of the correlation coefficient (as indicated by small circles in the figures) occurs is employed as the compromised length of the time window, which guarantees the integrity of the statistics and simultaneously meets the requirement of present application.

4. Examination of the proposed technique

The proposed technique was extensively verified by experiments before it was applied to practical applications. In the following, an illustrative example is given in order to show the effectiveness of the proposed technique in improving the accuracy of the CWT and its robust noise rejection performance. The simulated signal used in the example is

$$X(t)=8\mathrm{e}^{-\tilde{t}/25}\sin(\omega_0\tilde{t})+\sum_{i=1}^{4}\sin(\omega_i t)+n(t), \tag{17a}$$

where $n(t)$ indicates white noise. $\omega_0=2\pi f_0$, $\omega_i=2\pi f_i$,

$$\tilde{t}=\begin{cases} t & (0\leqslant t/t_0<1),\\ t-Nt_0 & (N\leqslant t/t_0<N+1)\end{cases} \tag{17b}$$

and N is a positive integer.

When t changes from 0 to 0.5 s, $t_0=0.05$ s, $f_0=600$ Hz, $f_i=i\times 100$ Hz and $n(t)=0$, the time waveform of the signal is shown in Fig. 2, where the sampling frequency of the signal is 2 kHz.

In this test, the signal is analysed by using the proposed technique. In the meantime, the traditional CWT and a few available purification methods such as the wavelet ridge extraction method [14], Donoho's method [15], and Yang's method [16] are also used to analyse the signal for comparison. All analysed results are shown in Fig. 3.

According to Eq. (17), the signal contains five frequency components, i.e. 100, 200, 300, 400 and 600 Hz. As Fig. 3(a) shows, the traditional CWT identifies them correctly. However, their time–frequency features are

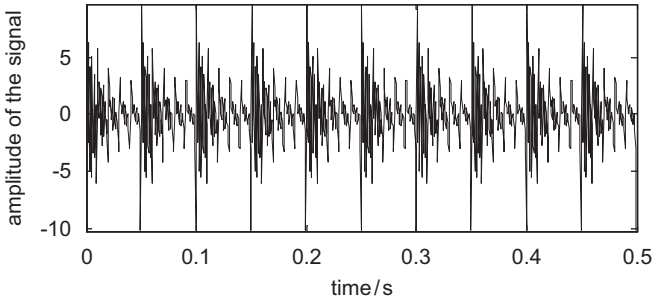

Fig. 2. The simulated signal used in the test.

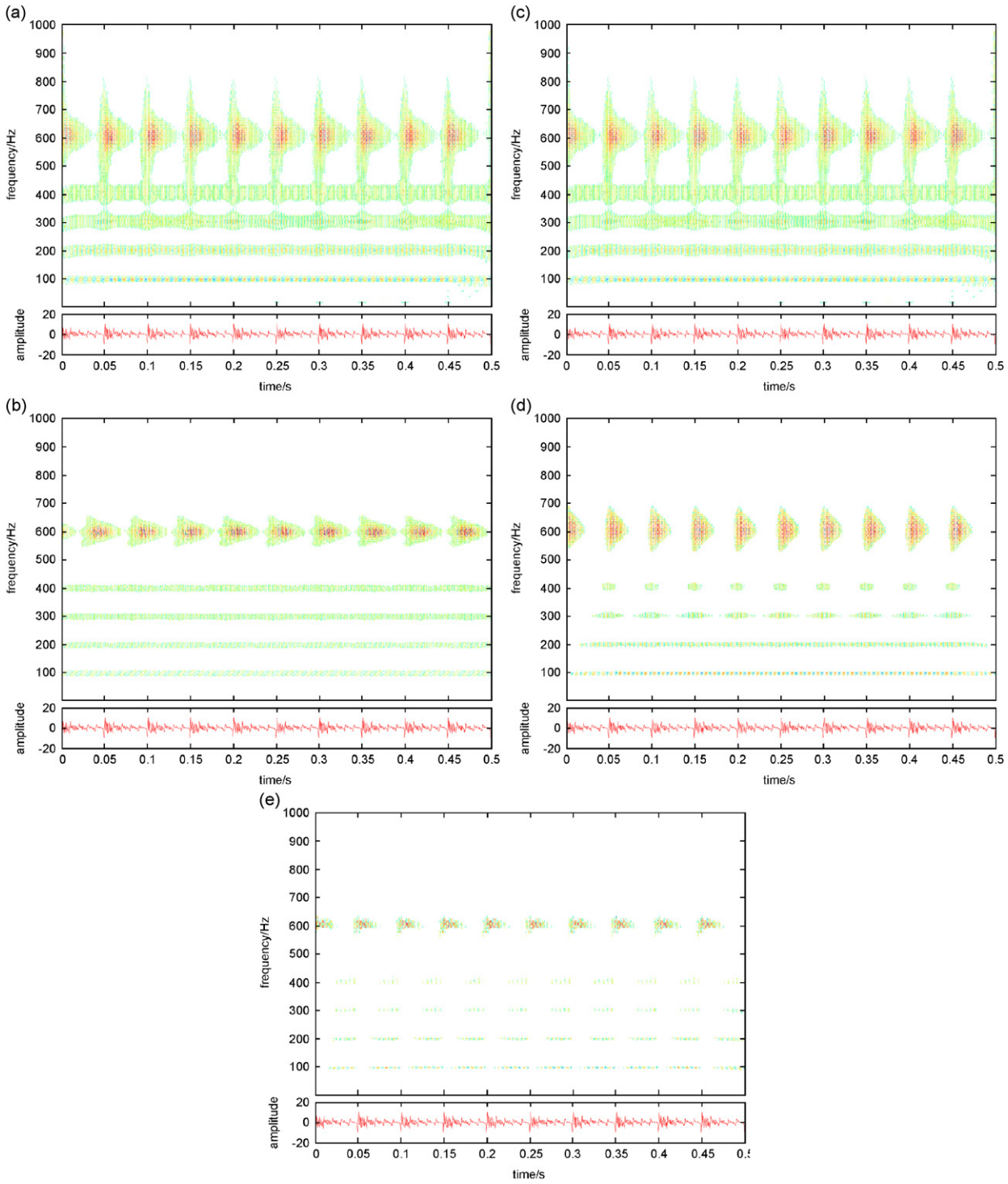

Fig. 3. Comparison of the proposed technique, the traditional CWT and its available purification methods: (a) results by traditional CWT, (b) results by proposed technique, (c) trimmed CWT by Donoho's approach, (d) wavelet ridge extraction method, and (e) trimmed CWT by Yang's soft-threshold method.

smeared due to the overlapping in their frequency vicinities. As Donoho's approach was designed mainly for the purpose of noise cancellation, no apparent improvement can be found from Fig. 3(c) as the signal is a pure signal and does not contain any noise in it. Figs. 3(d) and (e) show that after using the wavelet ridge extraction method and especially after using Yang's soft-threshold method, the time–frequency features in the CWT map become more explicit. However, their continuity and smoothness are seriously disrupted and moreover, part of true information of the signal are wrongly removed by mistake. In contrast, from Fig. 3(b), it is observed that after using the proposed technique, not only the undesired overlapping phenomenon in the CWT map is successfully removed and simultaneously the true information is sufficiently retained, but also the smoothness and the continuity of the wavelet coefficients are maintained perfectly. So the derived results are more reliable than those derived by using the wavelet ridge extraction method and Yang's soft-threshold method.

Subsequently, the robust noise performance of the proposed technique is examined. Two low levels of the signal-to-noise ratio (SNR), 5 and 1 dB, are considered in the examination. The examination results are shown in Fig. 4.

From Fig. 4, it is observed that due to the interference of white noise, the signal features in the CWT map are seriously smeared and diluted. Moreover, it is found that the smaller the SNR, the worse the situation tends to be. After adopting the proposed technique to trim the CWT map, the negative influence of the white noise is relieved dramatically, while the true information of the signal is retained sufficiently. The signal features still can be easily identified even when the SNR is as low as 1 dB. This experiment fully demonstrates

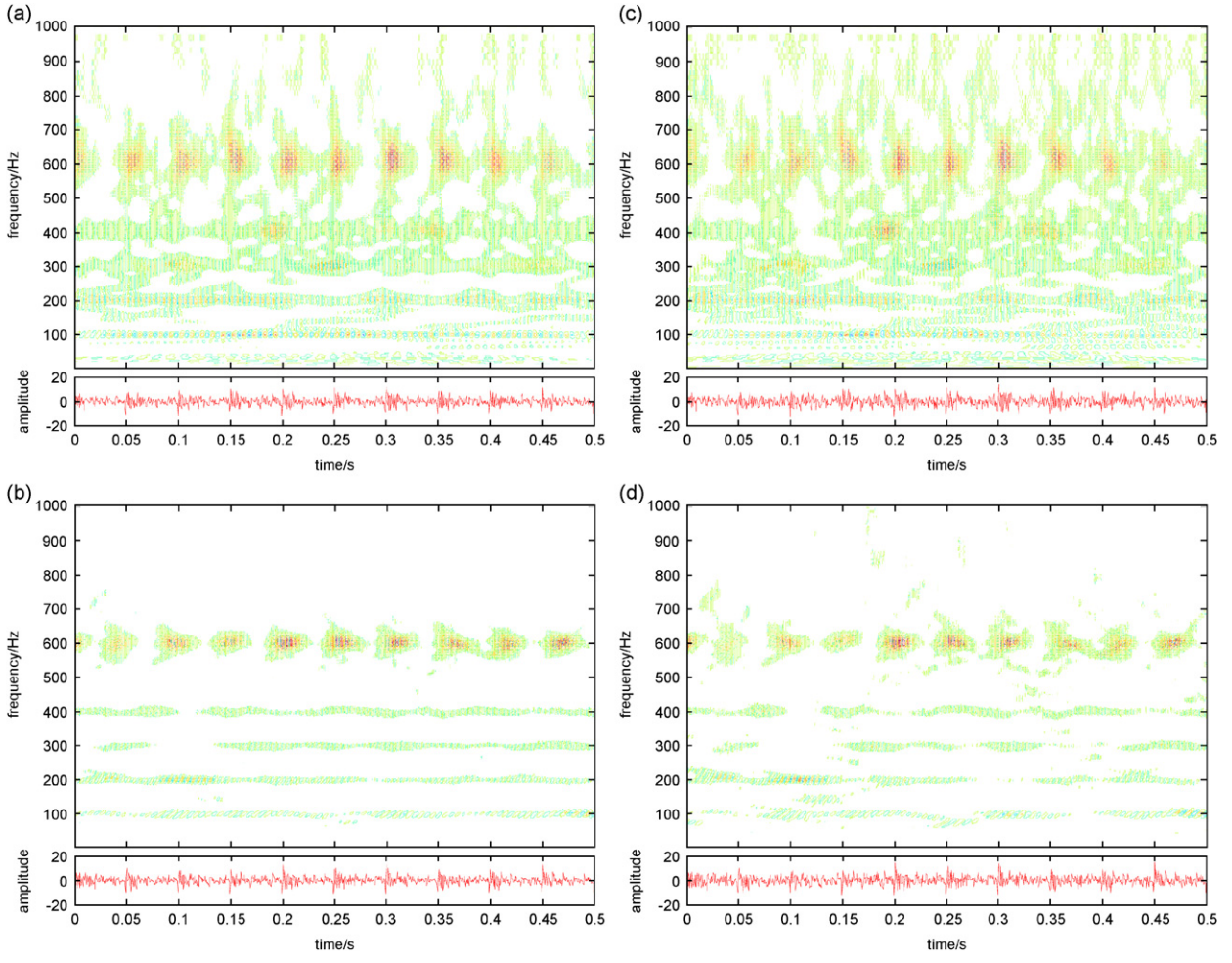

Fig. 4. Examination of the robust noise performance of the proposed technique: (a) traditional CWT when SNR = 5 dB, (b) proposed technique when SNR = 5dB, (c) traditional CWT when SNR = 1dB, and (d) proposed technique when SNR = 1 dB.

that the proposed technique possesses strong robust performance against the influence of white noise. It can be applied to dealing with those signals collected under aggressive environmental conditions.

Based on the experiments described above, we may say that the proposed technique does work in improving the accuracy of the CWT analysis and moreover shows more advantages in practical applications in comparison with other available techniques.

5. Practical application of the proposed technique

In this section, the vibration signals collected from an engine valve are analysed by using both the proposed technique and the traditional CWT for showing the successful application of the proposed technique in industry.

As depicted in Ref. [17], for a six cylinders, four stroke diesel engine, the normal valve-tappet clearance of the exhaust valves is 0.1 mm. A severe valve clearance fault was simulated by adjusting the clearance to 0.5 mm. The vibration signals collected from the valve tip before and after this adjustment are shown in Fig. 5. Obviously, it is hard to assess the change of valve condition directly from the signal waveforms. But the FFT spectra of the signals show that the vibration energy of the valve moves towards the high frequency region

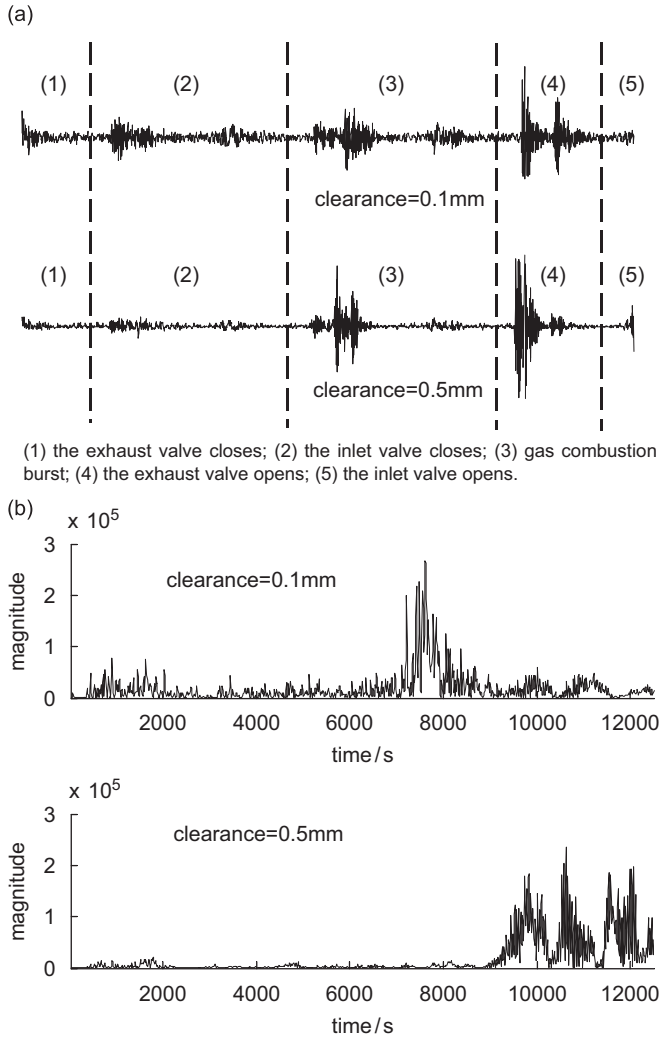

Fig. 5. Vibration signals collected from Engine valve: (a) time waveforms of the signals, and (b) FFT spectra of the signals.

when the clearance is abnormal. This information is very useful for monitoring the running condition of the valve.

In the following, the time–frequency features of the signals are analysed by using the CWT approaches. The results derived by using both the traditional CWT and the proposed technique are shown in Fig. 6. In the meantime, the short-time Fourier transform (STFT) spectra of the signals are also shown in the figure for verification purpose.

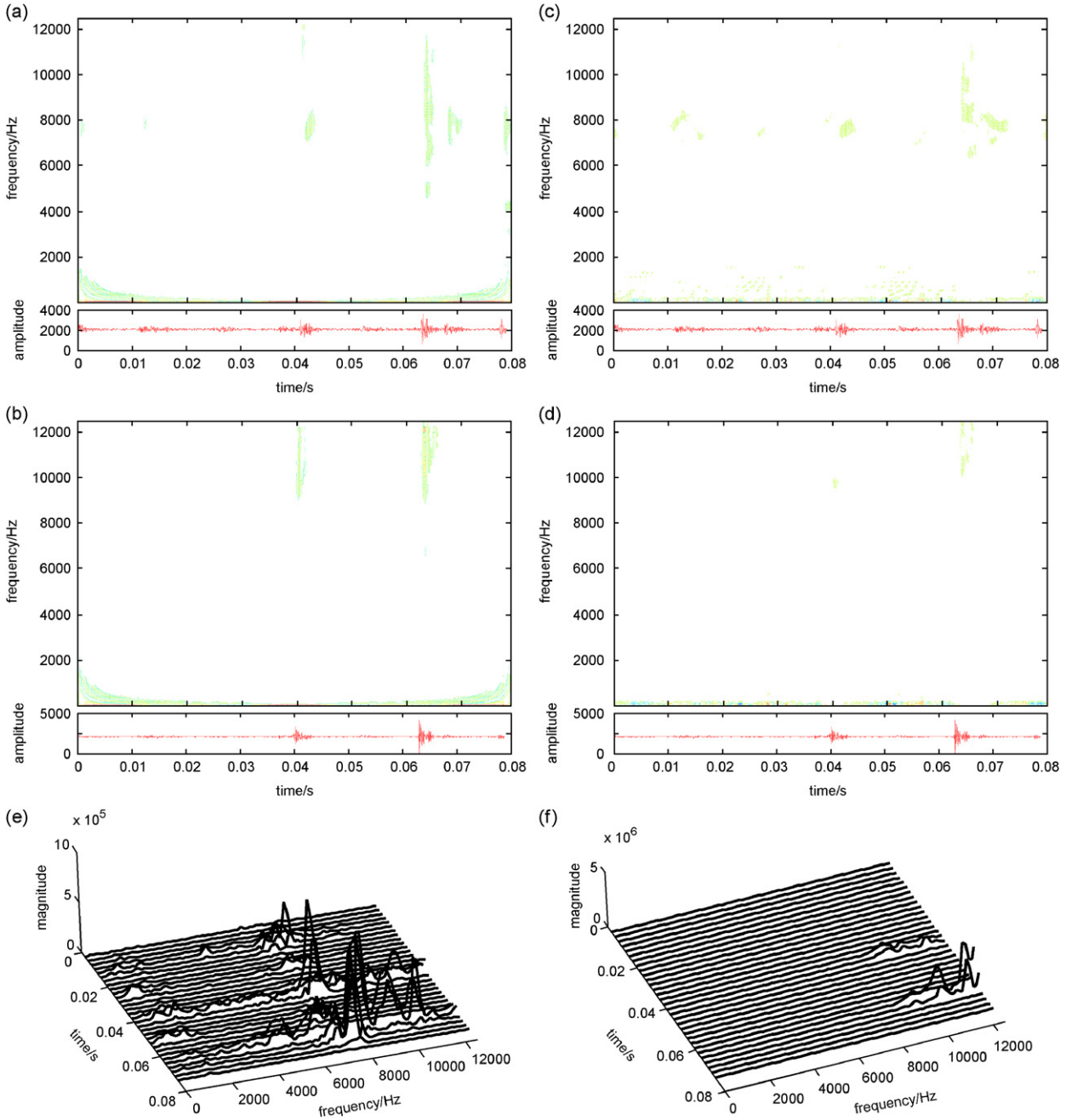

Fig. 6. Analysis of engine valve signals: (a) traditional CWT, clearance = 0.1 mm, (b) traditional CWT, clearance = 0.5 mm, (c) proposed technique, clearance = 0.1 mm, (d) proposed technique, clearance = 0.5 mm, (e) STFT, clearance = 0.1 mm, and (f) STFT, clearance = 0.5 mm.

From Fig. 6, it is obviously found that the proposed technique gives a more accurate description of the signal features in both the time and frequency domains. When the clearance is 0.1 mm, the proposed technique not only allocates the principal vibration energy of the valve accurately, but also gives a correct description of the low frequency energy of the valve. The correctness of this conclusion may be confirmed by the STFT spectra of the signals. In contrast, the traditional CWT fails to describe the distribution of low frequency energy and moreover does not give a satisfied description of the distribution of the principal valve energy in the frequency domain. After the clearance is wrongly adjusted to 0.5 mm, the redistribution of valve energy may be observed from the maps derived by using both methods. But reference to the FFT spectra shown in Fig. 5 and the STFT spectra shown in Fig. 6 demonstrates that traditional CWT does not give a very correct description of the energy distribution. For example, the energy around 6 kHz appears in the CWT map. Obviously, that is a false information created by overlapping. In comparison, the proposed technique gives an accurate and perfect description of the energy distribution. There is not any false information appearing in the map. Simultaneously, the true information of the signal is successfully retained and allocated correctly in both the time and frequency domains.

6. Concluding remarks

In view of the problem of the traditional CWT and the shortcomings of those CWT purification methods available now such as Donoho's approach, the wavelet ridge extraction method and Yang's soft-threshold method, a new technique is developed in this paper for further improvement of the accuracy of the CWT analysis. Both the fundamental theory and the examinations of the proposed technique are depicted in detail in this paper, through which the following conclusions are reached.

(1) The proposed technique discriminates the role of different scale of the daughter wavelet in the CWT process and trims the CWT coefficients according to the role of the present daughter wavelet at current time instant. Attributed to this delicate trimming strategy, both the true and false information in the CWT results are dealt with correctly. In contrast, the threshold-based methods do not discriminate the role of different scales of daughter wavelets. They trim the CWT through the approach of the threshold. In consequence, they often eliminate true information by mistake and incorrectly retain the false information in their results.
(2) As the proposed technique trims the CWT coefficients in a natural way by referring to the role of the daughter wavelet, the smoothness and the continuity of the wavelet coefficients are sufficiently maintained. In comparison, the smoothness and the continuity of the wavelet coefficients are usually disrupted by the threshold-based methods. Thus, the results derived by using the proposed technique are more reliable.
(3) In the implementation of the proposed technique, the frequency of the sinusoidal function and the length of time window used for correlation calculation may be easily determined and moreover, their determination may be realized intelligently through a simple computer programme. In contrast, an optimised threshold and the parameters used in threshold-based techniques can hardly be determined through an intelligent way. Contrarily, manual involvement is often required in the process.
(4) By using the proposed technique, almost all noise-induced structures are correctly removed from the CWT map because the noise is always unrelated to the true information contained in the inspected signal. Therefore, the proposed technique possesses a strong noise robust performance. It can be applied to dealing with those vibration signals colleted in aggressive environmental situations.
(5) Attributed to the aforementioned advantages of the proposed technique, the proposed technique always brings us with explicit spectral features in the CWT map, which significantly improves the accuracy of the CWT analysis. This approach could be very helpful in promoting better understanding of dynamical behaviour in practical applications.

Acknowledgements

This research work was supported by the National Natural Science Foundation of China (Ref. No. 50205021) and the Shaanxi Provincial Natural Science Foundation (Ref. No. $2002E_226$). In the meantime, the author would like to express his sincere appreciation to the reviewers for their comments and revisions on this paper.

References

[1] J. Morlet, Sampling theory and wave propagation, in: C.H. Chen (Ed.), *Acoustic Signal/Image Processing and Recognition, No. 1 in NATO ASI*, Springer, New York, 1983, pp. 233–261.

[2] I. Daubechies, *Ten Lectures on Wavelets, in CBMS-NSF Regional Conference Series in Applied Mathematics*, Vol. 61, SIAM, Philadelphia, PA, 1992.

[3] C.K. Chui, *An Introduction to Wavelets*, Vol. 1, Academic Press, San Diego, CA, 1992.

[4] B. Jawerth, W. Sweldens, An overview of wavelet based multiresolution analysis, *SIAM Review* 36 (3) (1994) 377–412.

[5] G. Strang, T. Nguyen, *Wavelet and Filters Bank*, Welsley-Cambridge, Cambridge, 1996.

[6] J.P. Antoine, R. Murenzi, P. Vandergheynst, S.T. Ali, *Two-Dimensional Wavelets and their Relatives*, Cambridge University Press, Cambridge, 2004.

[7] H. Kim, H. Melhem, Damage detection of structures by wavelet analysis, *Engineering Structures* 26 (2004) 347–362.

[8] P.W. Tse, W.X. Yang, H.Y. Tam, Machine fault diagnosis through an effective exact wavelet analysis, *Journal of Sound and Vibration* 277 (2004) 1005–1024.

[9] W.J. Wang, P.D. Mcfadden, Application of wavelets to gearbox vibration signals for fault detection, *Journal of Sound and Vibration* 192 (1996) 927–939.

[10] W.X. Yang, J.B. Hull, M.D. Seymour, A contribution to the applicability of complex wavelet analysis of ultrasonic signals, *NDT & E International* 37 (2004) 497–504.

[11] M.N. Ta, J. Lardiès, Identification of weak nonlinearities on damping and stiffness by the continuous wavelet transform, *Journal of Sound and Vibration* 293 (2006) 16–37.

[12] P. Tse, W.X. Yang, A new wavelet transform for eliminating problems usually occurring in conventional wavelet transforms used for fault diagnosis, The Ninth International Congress on Sound and Vibration, ICSV'9, Orlando, FL, Paper No. 465, CD-ROM version, 2002.

[13] P. Tse, W.X. Yang, The practical use of wavelet transforms and their limitations in machine fault diagnosis, *International Symposium on Machine Condition Monitoring and Diagnosis*, Invited paper, Tokyo, Japan, 2002. pp. 9–16.

[14] D.E. Newland, Ridge and phase identification in the frequency analysis of transient signals by harmonic wavelets, *Transaction of ASME Journal of Vibration and Acoustics* 121 (1999) 149–155.

[15] D.L. Donoho, De-noising by soft-thresholding, *IEEE Transactions on Information Theory* 41 (3) (1995) 613–627.

[16] W.X. Yang, P. Tse, An advanced strategy for detecting impulses in mechanical signal, *Transaction of ASME Journal of Vibration and Acoustics* 127 (2005) 280–284.

[17] W.X. Yang, Establishment of the mathematical model for diagnosing the engine valve faults by genetic programming, *Journal of Sound and Vibration* 293 (2006) 213–226.